

Artificial Gravity Visualization, Empathy, and Design

Theodore W. Hall*
<http://www.twhall.com/>

Artificial gravity is well known and understood in abstract mathematical terms, but not in terms of a pervasive life condition. To design comfortable artificial gravity habitats, architects must have some empathy for the people who will inhabit them. Visualization is the first step toward developing that empathy. Flaws in published design concepts are evidence of the inadequacy of past visualizations. This paper presents visualizations that reveal those flaws, to promote general guidelines for better design of artificial-gravity habitats. These visualizations reveal that conformance to the “comfort zone” for artificial gravity does not guarantee an Earth-like gravitational environment. They aim to help architects recognize important design constraints beyond the basic rotational parameters. In particular, the Coriolis effects associated with movement in a rotating environment impose specific north-south and east-west axes, in addition to the up-down axis. Axially symmetric plans that ignore the orientation of Coriolis effects are not well adapted to life in artificial gravity, especially at small radii.

Nomenclature

A	=	acceleration
A_{cent}	=	centripetal acceleration (nominal artificial gravity)
A_{Cor}	=	Coriolis acceleration
R	=	radius of rotation
V	=	tangential velocity (rim speed) of habitat
v	=	relative velocity of inhabitant perpendicular to the habitat’s axis of rotation
Ω	=	angular velocity of habitat

I. Introduction

From the earliest conceptions, beginning with Konstantin Tsiolkovsky more than a hundred years ago, space station design featured artificial gravity as the most important determiner of form. Early visionaries regarded micro-gravity as a dangerous or inconvenient curiosity, unrelated to the mission of the station. The mission was to be Earth observation, astronomy, logistic support of trans-planetary excursions, or national defense.

Only after more than a decade of gradually increasing human exposure to micro-gravity did it finally supplant artificial gravity in space station design – and not for the sake of crew safety or convenience, but primarily as a cost-saving measure. Though many now regard access to micro-gravity as a principal research mission of the International Space Station, much of the life science aspect of that research would be moot if the station provided artificial gravity; the research is quite introspective.

With renewed planning for human excursions to other planets, with transit times measured in months and round-trip travel measured in years, there is a renewed interest in artificial gravity. In transiting to Mars, long exposure to micro-gravity is dangerous and inconvenient; it is not a mission objective, and hopefully not a necessity.

Artificial gravity is well known and understood in abstract mathematical terms, but not in terms of a pervasive life condition – not in the way that Earth’s natural gravity is known and understood. Terrestrial architects routinely design for life in Earth’s one g, using common sense developed from direct experience and backed up by design precedents that have evolved through millennia of trial and error. Whether explicit or not, considerations of gravity pervade nearly every aspect of terrestrial design. Most architects designing for non-terrestrial gravity regimes have neither experience nor many precedents to draw from. This is especially true for artificial gravity, which no human has ever experienced in its pure form, uncoupled from Earth’s one g. There is no common sense and no built precedent.

* Independent researcher, AIAA Member.

Governing standards such as NASA-STD-3000 are legalistic documents that mandate myriad individual responses to a plethora of special concerns. Reliance on such rules does not substitute for a deep pervasive understanding of the situation. One cannot learn to design merely by reading building codes. In any case, NASA-STD-3000 has very little to say about artificial gravity [NASA, 1995 July].

Before architects can design comfortable, functional artificial gravity habitats, they must develop some empathy for the people who will inhabit them. Perhaps this empathy can arise only from direct experience of similar conditions. That leaves us with a “chicken or egg” dilemma in designing the first such habitats. We must begin with some simulation and partial experience, such as visualization. Gravity and acceleration are experienced primarily through the vestibular and haptic senses, and secondarily through vision. However, visual sensations are much easier to generate, record, broadcast, and reproduce in media such as this.

Section II below reviews comfort charts, which are well-known and often-cited visualizations of the numerical parameters of artificial gravity. They’ve been important references in the design of these environments, but they’re too abstract to impart any empathy for living under such novel conditions. This section also describes an artificial-gravity calculator that assists in finding a set of parameter values within an agreed comfort zone.

Section III describes a dynamic graphic simulation of free-falling particles in artificial gravity, and illustrates how still frames from such a simulation can contribute to the visual evaluation of these environments. Gravity, whether natural or artificial, is manifest through its effect on free-falling particles.

Section IV describes the use of catenary curves to visualize the apparent slopes of straight chords in artificial gravity. This is especially important in the design of ladders and segmented floors. The orientation of a ladder with respect to the rotation is a critical design detail that often seems to be ignored in renditions of artificial-gravity habitats.

Section V discusses the potential of computer aided design and virtual reality to advance the visualization of artificial-gravity environments.

Section VI concludes with some general guidelines for the design of artificial-gravity environments based on these visualizations.

II. Comfort Charts and Calculators

The dawn of government-funded space station planning in the 1960’s included research into the comfort conditions for human habitation of artificial gravity. This began as an outgrowth of centrifuge studies on military pilots who needed to endure high g loads during maneuvers. While those military studies focused on high intensity and short duration, space station studies focused on low intensity and long duration. In the USA, much of this research occurred at the Naval Aviation Medical Acceleration Laboratory (US Naval Air Development Center, Johnsville, Pennsylvania), the Naval Aerospace Medical Research Laboratory (Pensacola, Florida), and the Rotating Space Station Simulator at NASA Langley Research Center (Hampton, Virginia).

In 1962, Hill and Schnitzer published one of the earliest and best-known visualizations of the “comfort zone” for artificial gravity, shown in Figure 1 [Hill, Schnitzer, 1962]. This chart circulated widely in the pages of the journal *Astronautics* and was still reappearing up to twenty-five years later in at least three separate papers [Schultz, Rupp, Hajos, Butler, 1989; Staehle, 1989; Tillman, 1987].

A little essential algebra determines the features of this chart. Tangential velocity (V) and centripetal acceleration (A_{cent}) depend on radius (R) and angular velocity (Ω) according to the following formulas:

$$V = \Omega \cdot R$$

$$A_{cent} = \Omega^2 \cdot R$$

(For numerical equality, Ω must be expressed as radians per time, V as distance per time, and A_{cent} as distance per time-squared.) In logarithmic form, these become:

$$\log(V) = \log(\Omega) + \log(R)$$

$$\log(A_{cent}) = 2 \cdot \log(\Omega) + \log(R)$$

Hill and Schnitzer measure $\log(R)$ on the vertical axis and $\log(\Omega)$ on the horizontal axis. Rewriting the last two relations above in the slope-intercept form ($y = m \cdot x + b$), they become:

$$\begin{aligned}\log(R) &= -\log(\Omega) + \log(V) \\ &= -2 \cdot \log(\Omega) + \log(A_{cent})\end{aligned}$$

Thus, contours of tangential velocity V have a slope of -1 while contours of centripetal acceleration A_{cent} have a slope of -2 . Using logarithmic rather than linear scales renders these contours as straight lines rather than curves.

Hill's and Schnitzer's hypothetical "comfort zone" is sandwiched between minimum and maximum centripetal accelerations of 0.035 g and 1.0 g (0.343 m/s^2 and 9.81 m/s^2). The lower bound seems to be an arbitrary value on their logarithmic scale. The zone is further bounded on the right by a maximum angular velocity of 4 rpm ($0.419\text{ radians per second}$). The value is documented in their article but not clearly labeled in their chart. This is to limit dizziness from "cross-coupled" head rotations. Another boundary, on the bottom-left, is a minimum tangential velocity of $20\text{ feet per second}$ (6.1 m/s) so that a person's relative velocity v within the rotating habitat doesn't affect the net apparent gravity too much. (The ratio of v/V should be small.) Finally, another potential boundary at the bottom is minimum radius. If the head-to-foot gravity gradient for a 6-foot person is limited to 12% , then $6/R \leq 0.12$ and $R \geq 50\text{ feet}$ (15.2 m). The chart indicates this with a horizontal dashed line just above the bottom tip of the shaded area. A greater tolerance for gravity gradient, allowing a smaller radius, is superseded by the intersection of the limits on maximum angular velocity and minimum tangential velocity. There are no explicit limits for maximum radius or minimum angular velocity: the bigger and slower the rotation, the better.

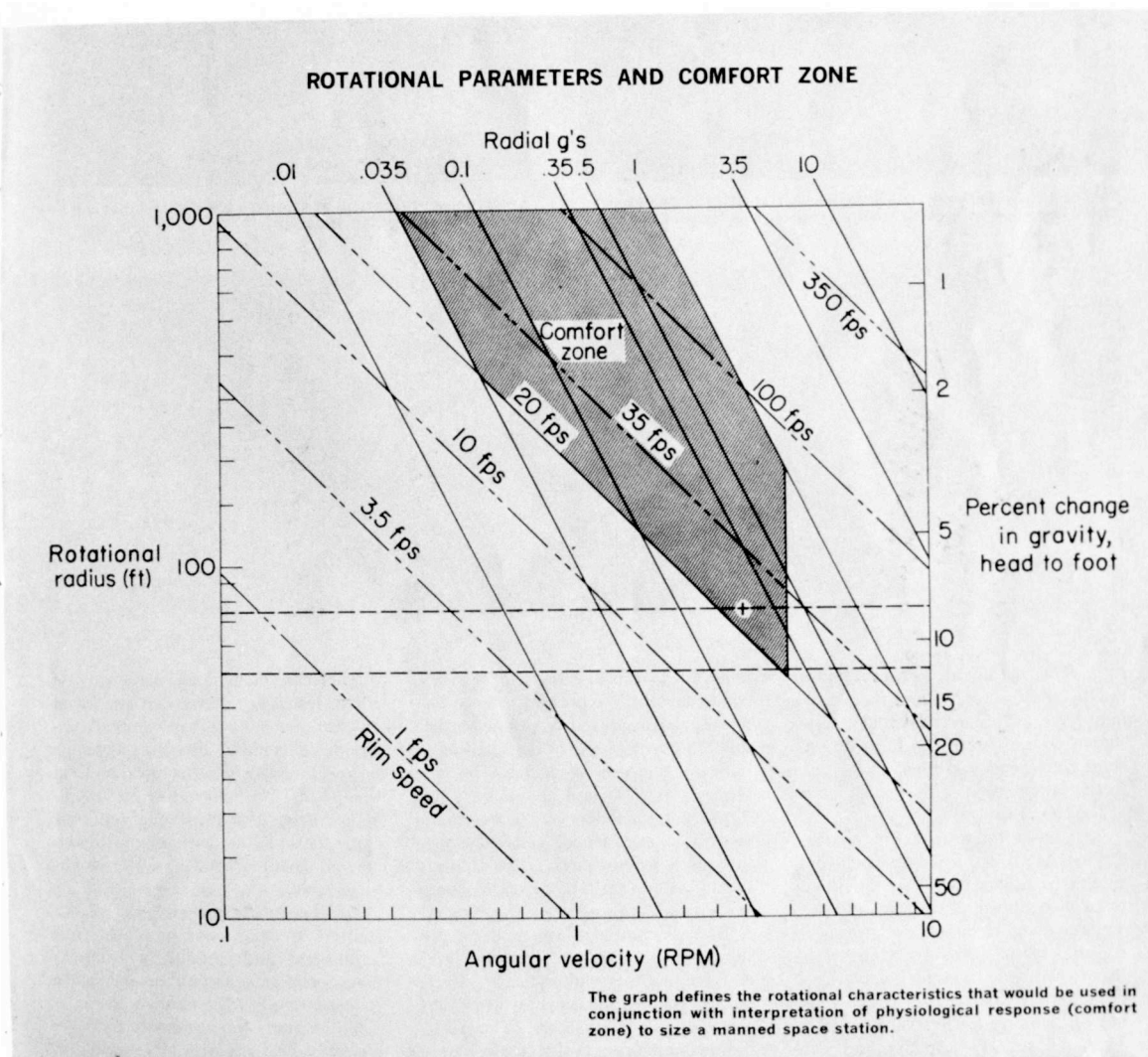


Figure 1. Comfort chart, Hill and Schnitzer, 1962.

This is not really a visualization of artificial gravity per se, but rather of mathematical relationships between numeric parameters. Charts such as this could just as well represent countless physical concepts unrelated to artificial gravity. For example, if the axes represented mass (m) and velocity (v), then the sloping contours would represent momentum ($m \cdot v$) and kinetic energy ($m \cdot v^2/2$). If the axes represented linear load density (w) and beam length (l), then the sloping contours would represent shear ($w \cdot l/2$) and bending moment ($w \cdot l^2/8$). Any chart that can represent all of these concepts can't represent any of them very specifically. It's not an adequate visualization for developing any particular feel for artificial gravity. It visualizes the math, but not the physical phenomenon.

Hill's and Schnitzer's comfort chart is neither the latest nor necessarily the best. Figures 2 through 5 show alternatives published by Gilruth [1969], Gordon and Gervais [1969], Stone [1973], and Cramer [1985]. The first thing one might notice in trying to compare these charts is how incomparable they are. No two of them are formatted quite the same. The inconsistent formats veil significant disagreements regarding the limits of the comfort zone. In fact, no two of the charts agree on all of the limits.

Gilruth's chart, shown in Figure 2, uses linear rather than logarithmic axes, with centripetal acceleration on the vertical axis. Contours of radius appear as a set of parabolas, with steeper curves corresponding to larger radii. A maximum head-to-foot gravity gradient of 15% implies a minimum radius of 40 feet (12.2 m), which clips across the lower-right corner of the comfort zone. The minimum and maximum centripetal accelerations are 0.3 g and 0.9 g (2.94 m/s^2 and 8.83 m/s^2). Setting the upper limit less than 1 g may be to allow for some inevitable Coriolis acceleration without pushing the net acceleration above 1 g. The chart distinguishes between "comfort" and "optimum comfort", limited by maximum angular velocities of 6 rpm and 2 rpm respectively (0.628 and 0.209 radians per second). There's no indication of any limit on tangential velocity.

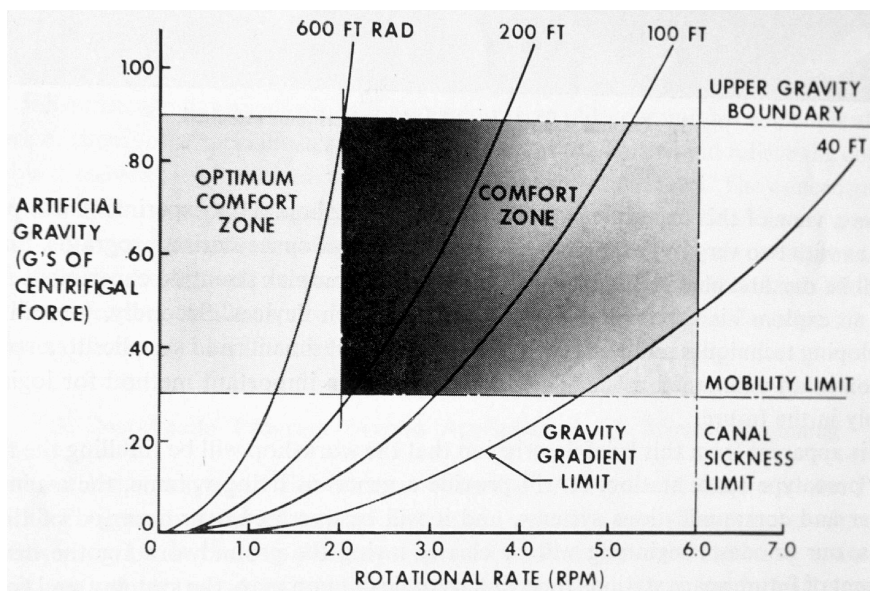


Figure 2. Comfort chart, Gilruth, 1969.

Gordon's and Gervais's chart, shown in Figure 3, is the most similar to Hill's and Schnitzer's. It adopts essentially the same logarithmic format, but swaps the horizontal and vertical axes. It also indicates higher limits for nearly every parameter. The minimum centripetal acceleration is 0.2 g (1.96 m/s^2). The maximum angular velocity is 6 rpm (0.628 radians per second). The minimum tangential velocity is 24 feet per second (7.3 m/s). There's no indication of any limit on gravity gradient or radius.

Stone's chart, shown in Figure 4, uses the same axis variables as Gordon's and Gervais's, but with linear rather than logarithmic scales; it measures Ω on the vertical axis and R on the horizontal axis. Because of the non-logarithmic scales, contours of tangential velocity and centripetal acceleration render as curves. The velocity contours are steeper than the acceleration contours, especially at the left. The curve that delimits the bottom-left of the comfort zone corresponds to a tangential velocity of about 10.2 m/s. A horizontal line marks a maximum angular velocity of 6 rpm. Vertical lines mark limits on radius based on the gravity gradient and the deflection of dropped objects. But again, these limits are superseded by the intersection of the limits on maximum angular velocity and minimum tangential velocity.

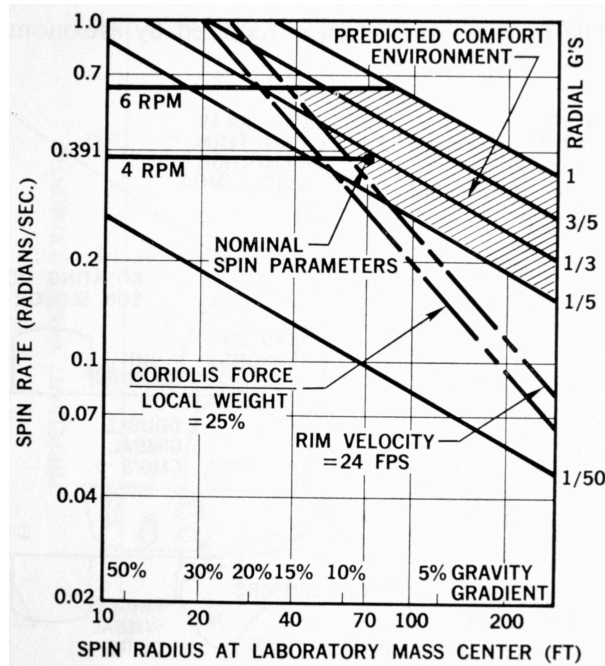


Figure 3. Comfort chart, Gordon and Gervais, 1969.

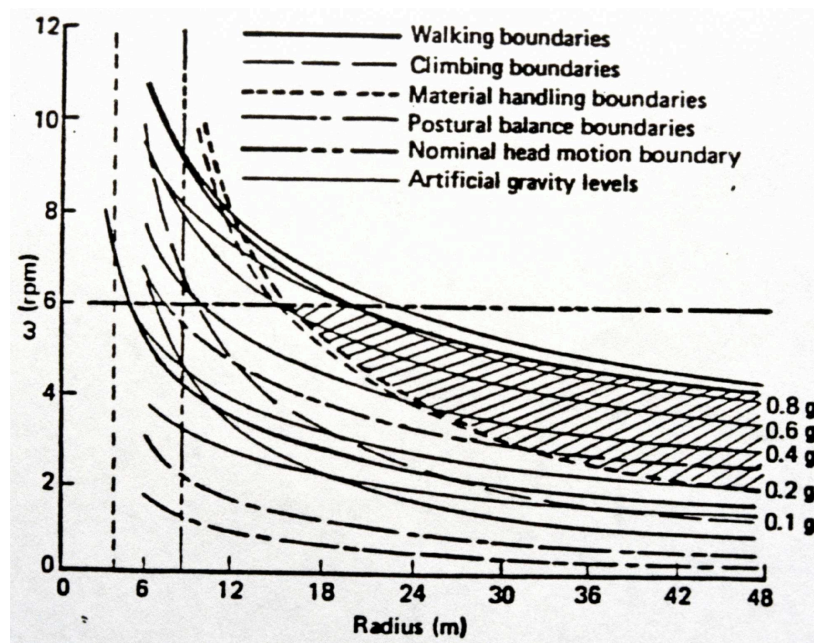


Figure 4. Comfort chart, Stone, 1973.

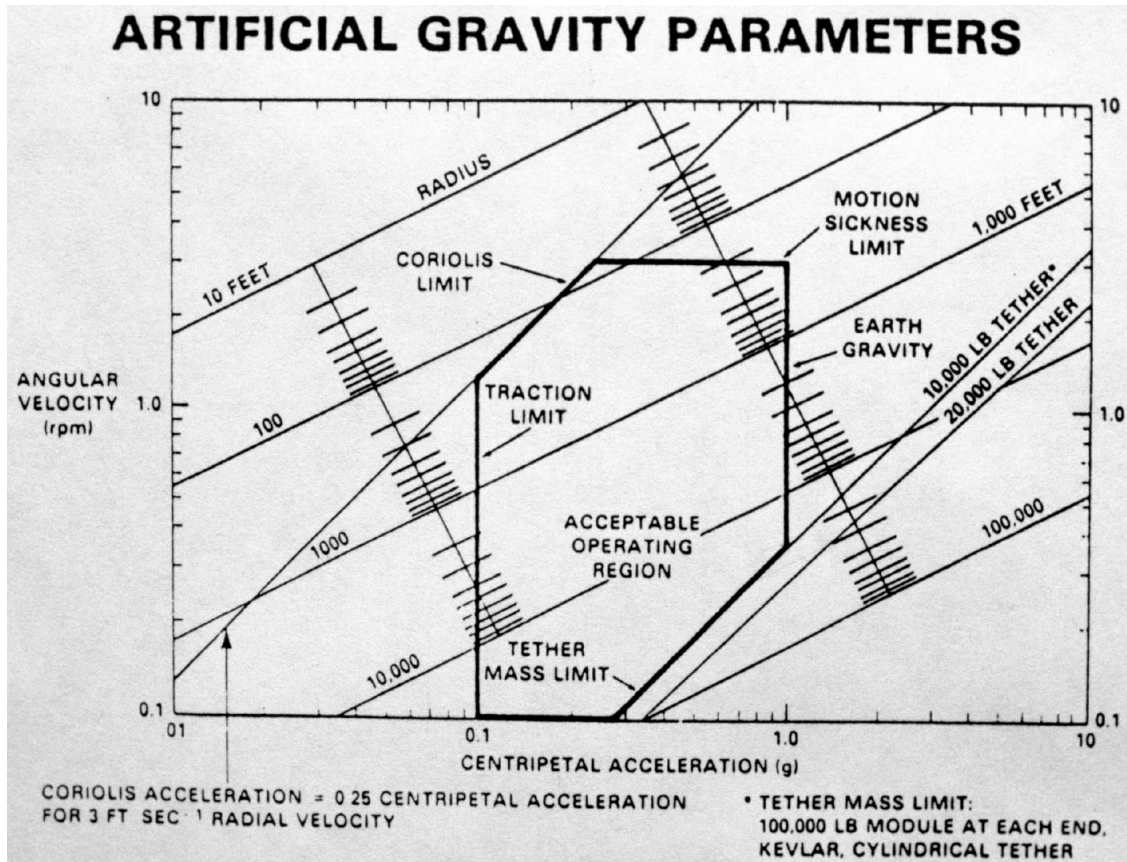


Figure 5. Comfort chart, Cramer, 1985.

Cramer's chart, shown in Figure 5, again uses logarithmic scales, but with $\log(\Omega)$ on the vertical axis and $\log(A_{cent})$ on the horizontal axis. The comfort zone is bounded on the left and right by minimum and maximum centripetal accelerations of 0.1 g and 1 g (0.981 m/s^2 and 9.81 m/s^2). On top, the zone is bounded by a maximum angular velocity of 3 rpm (0.314 radians per second). Contours of radius appear as lines with a slope of 1/2, while contours of tangential velocity appear as lines with a slope of 1. A boundary for minimum tangential velocity of 24 feet per second (7.3 m/s) clips across the top-left corner of the comfort zone. This boundary insures that the Coriolis/centripetal ratio will not exceed 0.25 for a radial velocity of 3 feet per second (0.91 m/s). A unique feature of this chart is a boundary for maximum tangential velocity, imposed not for human comfort but for the load capacity of tethers. (The self-weight of a cylindrical tether in artificial gravity is proportional to its centripetal acceleration and length, and $A_{cent} \cdot R = \Omega^2 \cdot R^2 = V^2$.) This limit is about 900 feet per second (274 m/s) and clips across the bottom-right corner of the comfort zone. The chart shows many contour values for radius, but none of them contributes anything to the comfort boundaries.

All of these charts suffer from the same fundamental weaknesses:

- They represent abstract mathematical relationships that are not unique to artificial gravity.
- They portray the comfort boundaries as precise algebraic relations, discarding the underlying statistics of means and deviations. Only when the charts are considered together – with considerable difficulty due to their disparate formats – do the uncertainties in the boundaries become apparent.
- They don't facilitate reading parameter values within the comfort zone, but instead seem to encourage the use of edge values on the frontiers of comfort.

Figure 6 begins to address the second weakness described above by compositing all of the alternative limits cited by these authors onto a single chart. The green zone depicts conditions that all agree are comfortable, requiring little adaptation. The red zone depicts conditions that all agree are not comfortable, even after a period of adaptation. The intermediate zones ranging through shades of yellow and orange depict areas of disagreement. Moving through these zones, away from the green and toward the red, demands greater adaptability of the inhabitants to the peculiar conditions of life in constant rotation.

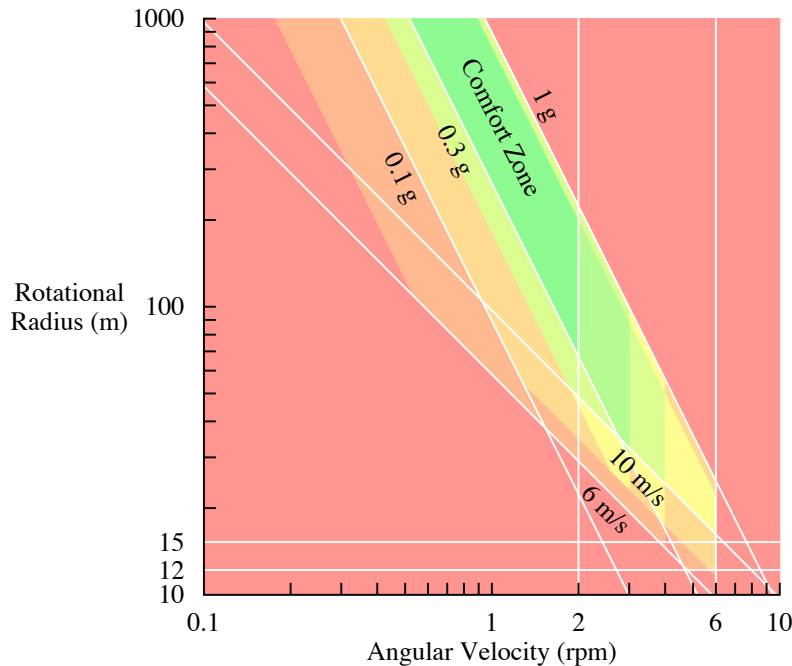



Figure 6. Comfort chart composited from Figures 1 through 5. The green zone depicts conditions that the cited authors agree are comfortable. The red zone depicts conditions that they agree are not comfortable. The intermediate zones ranging through shades of yellow and orange depict areas of disagreement.


Radius (R)



meters

$R \propto A/\Omega^2$


Angular Velocity (Ω)



rotations/minute

input


Tangential Velocity (V)



meters/second

$V \propto A/\Omega$

Centripetal Acceleration (A)



g

input

Figure 7. SpinCalc

determined that R must be 9.44 m and V must be 5.93 m/s. Although the input values for both Ω and A meet at least one set of comfort criteria when considered independently, when taken together they result in a V that's definitely too low. If the user now inputs a greater value for V , the calculator will recompute R and either Ω or A – whichever of the two was least recently input. Working back and forth among the parameters, the user can quickly arrive at a set of acceptable values.

Figure 7 addresses the third weakness of comfort charts. It illustrates SpinCalc, an artificial-gravity calculator that assists in finding a set of parameter values that conform to all of the comfort boundaries*. The four parameters – R , Ω , V , and A – are interdependent. The user may input any two, in any of several units selected from drop-down menus. The calculator computes the other two from the input. The text beneath each value indicates how the value was determined. The colored icon to the left of each value indicates its relationship to the presumed comfort boundaries for artificial gravity. Green indicates that all of the cited authors agree that the value is comfortable. Red indicates agreement that it is not comfortable. Yellow indicates disagreement. Up arrows indicate that the value should be greater; down arrows indicate that it should be less.

In this example, the user is checking design parameters for a hypothetical Earth-to-Mars transit habitat. He has guessed 6 rpm for Ω and 0.38 g for A , and entered these as input. The calculator has

* At <http://www.artificial-gravity.com/ag/sw/SpinCalc/>. Original coding 2000/01/27; last revision 2003/05/05.

III. Free-Falling Particles and Involute Curves

This section begins to address the first weakness cited above for comfort charts as visualizations of artificial gravity: their mathematical abstraction. Figure 8 illustrates SpinDoctor, an interactive dynamic graphic simulation of free-falling particles in artificial gravity*. The bottom-right quadrant is a control panel for specifying the initial height and velocity of a particle (in units of m, m/s, and degrees of elevation from east), and the rotational parameters R , Ω , and A (in units of m, rpm, and g). As in SpinCalc, the rotational parameters are inter-dependent. Specifying any two of them determines the third. Whenever the user changes one of them, the program recalculates another one – the one least recently specified by the user – so that the remaining parameter remains constant.

The top-right quadrant shows an inertial view of the situation. The top-left quadrant shows a rotating view, as experienced by an inhabitant of the rotating frame. The bottom-left quadrant shows the behavior of an identical particle thrown with the same initial height and velocity on Earth.

In this example, the habitat has a floor radius of 50 m and is rotating at 3 rpm for a centripetal acceleration of 0.5 g. Although all three parameters conform to most renditions of the comfort zone for artificial gravity, the particle's behavior under these conditions is profoundly different from its behavior on Earth. By adjusting the parameters and seeing the particle's motion in real time, the user may obtain some sense of the shape of the apparent artificial-gravity field and the meaning and significance of the comfort criteria.

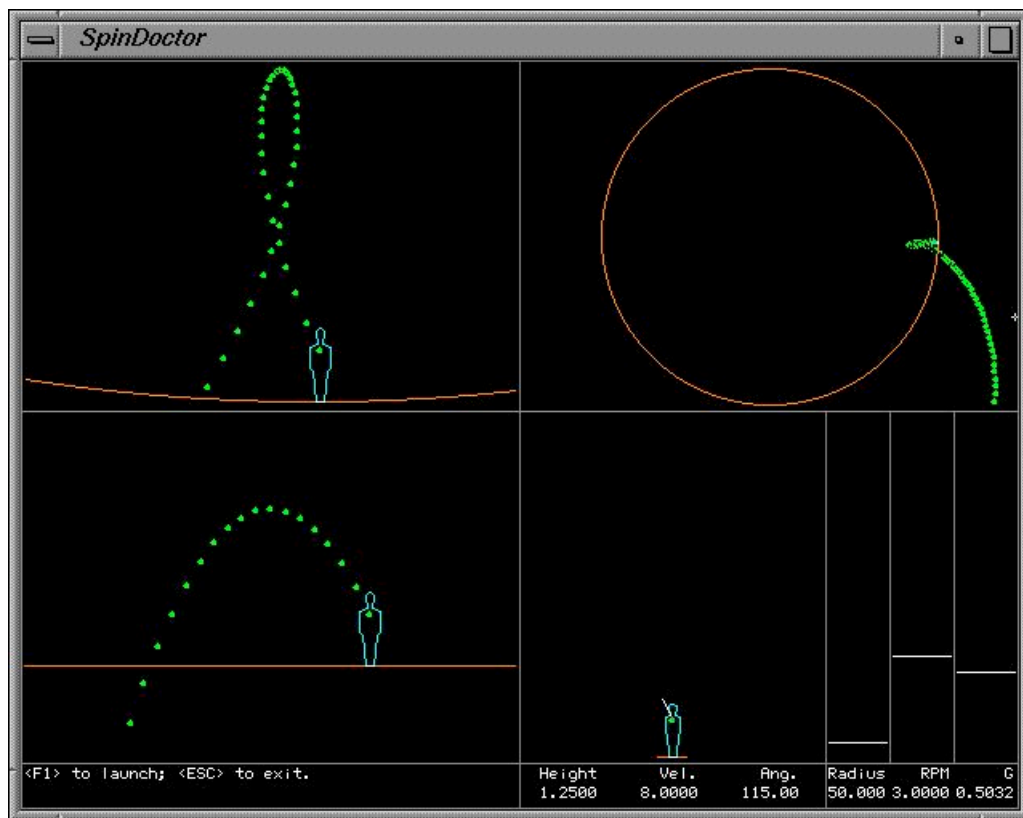


Figure 8. SpinDoctor

Observing the dynamic behavior of falling objects in real time may be the best way to gain an understanding of artificial gravity, short of actually living in it and feeling it through the vestibular and haptic senses. Unfortunately, the common technology for conference papers and design guides does not yet support embedded interactive real-time animations. Inasmuch as static printed books and papers (and their printable electronic equivalents) remain important media for communicating design information, still frames derived from such an animation have a role to play. These images must also be abstractions of the actual phenomenon, but perhaps they can be less abstract than comfort charts and easier to relate to physical experience.

* At <http://www.artificial-gravity.com/ag/sw/SpinDoctor/>. Original coding 1987/02/14; last revision 1999/06/22.

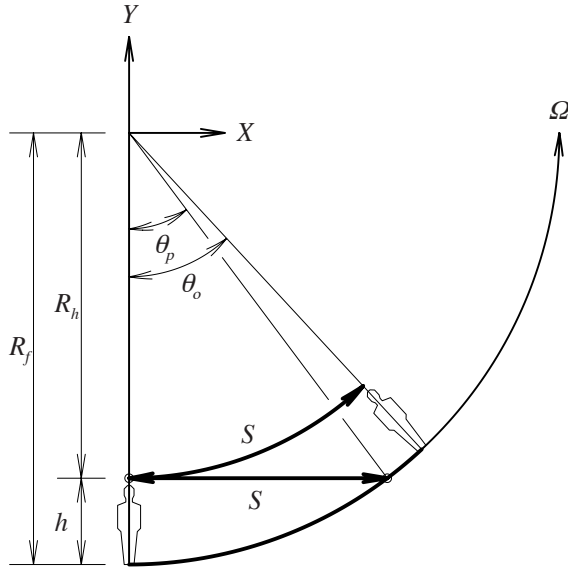


Figure 9. A dropping particle in artificial gravity.

Figure 9 shows the situation for a particle dropping from a height h above a floor with a radius R_f in an artificial-gravity environment. Contrary to popular misconception, there is neither any centrifugal force that pushes the particle toward the floor, nor any Coriolis force that diverts it. Rather, in the absence of any impinging force, the particle's momentum carries it at constant velocity through some distance S until it strikes the floor. If the particle had not been released, it would have traveled the same distance S along an arc. The falling particle subtends an angle θ_p while the observer, constrained to circular motion by centripetal force, subtends an angle θ_o :

$$R_h = R_f - h$$

$$S = \sqrt{R_f^2 - R_h^2}$$

$$\theta_p = \arctan(S/R_h)$$

$$\theta_o = S/R_h$$

Without delving into a lot of math, one can see in Figure 9 that the distances and angles are independent of the speed. One can imagine the animation running faster or slower, but the paths of the particle and the observer remain the same. This means that the relative path of the particle is independent of the angular velocity, tangential velocity, and centripetal acceleration. The shape of the path depends only on the ratio h/R_f .

If h is some defined proportion of human height, then one can see the importance of R_f as a design parameter: h is given by anthropometry and ergonomics; the designer's choice of R_f determines the relative deflection of particles falling from that height. The apparent gravity is most natural when the ratio h/R_f is small.

Figure 10 shows the relative paths of free-falling particles dropped from a certain initial height h , in artificial-gravity environments with various floor radii R_f . The straighter paths correspond to the smaller ratios of h/R_f . The curves are involutes: the particle follows a path like the endpoint of a thread unwinding from a spool. The "thread" is the inertial path of the particle, which Figure 10 renders for one case as a set of dashed lines. In the observer's frame of reference, the inertial path rotates. The path itself is invisible except for the particle at its endpoint.

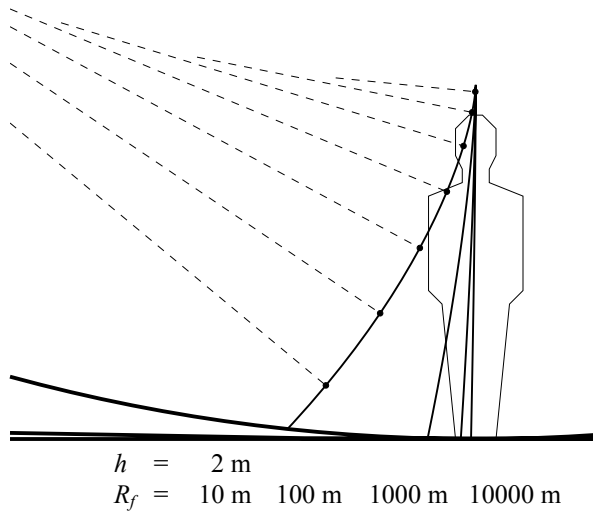


Figure 10. Dropping particles from an initial height h of 2 m. The shape of the path depends on the ratio h/R_f .

The apparent deflection of the particle, as seen by the rotating observer, is not due to Coriolis force, but rather due to the *absence* of the Coriolis force that would be required to constrain it to a straight line in the rotating frame of reference.

Figure 11 shows the situation for a particle hopping vertically from the floor with an initial relative velocity v . The inertial path cuts a chord across the circle with a slope equal to the ratio of the particle's relative hop velocity to the environment's tangential velocity: v/V . The proportions of the path depend only on that ratio, while its size depends on the circle's radius R_f . The velocity ratio v/V is also directly proportional to the ratio of Coriolis to centripetal acceleration, and so the shape of the path is indicative of that acceleration ratio:

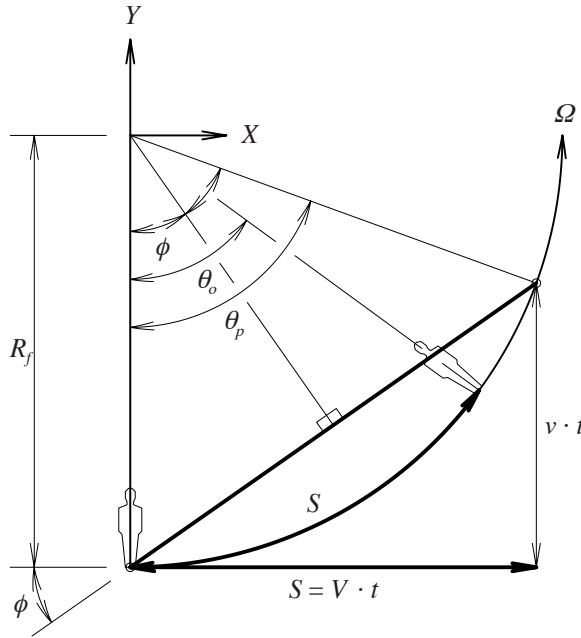


Figure 11. A hopping particle in artificial gravity.

$$\begin{aligned}\frac{A_{Cor}}{A_{cent}} &= \frac{2 \cdot \Omega \cdot v}{\Omega^2 \cdot R_f} \\ &= 2 \frac{v}{\Omega \cdot R_f} \\ &= 2 \frac{v}{V}\end{aligned}$$

Here, A_{Cor} is the Coriolis acceleration that would be required to maintain a constant relative velocity v on a straight path in the rotating frame of reference. Without that acceleration, the particle appears to deviate. A_{Cor} applies to any motion in the rotating frame perpendicular to the axis of rotation. Vertical “hopping” motion is just one example.

If v is some defined proportion of human speed, then one can see the importance of V as a design parameter: v is given by anthropometry and ergonomics; the designer’s choice of V determines the ratio of Coriolis to centripetal acceleration, and the relative deflection of particles launched with velocity v . The apparent gravity is most natural when the ratio v/V is small.

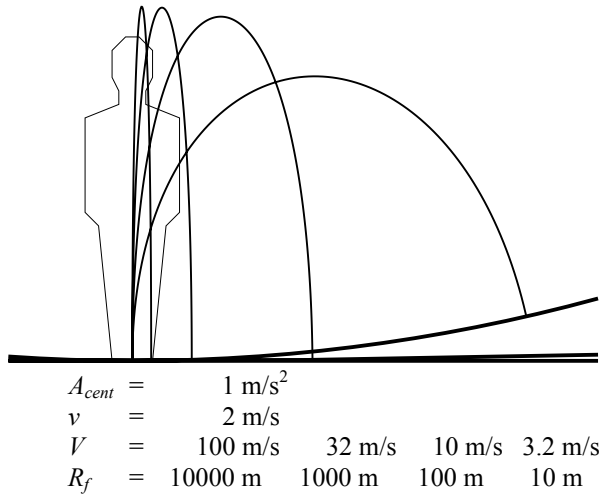


Figure 12. Hopping particles with an initial relative velocity v of 2 m/s and centripetal acceleration A_{cent} of 1 m/s² (about 0.1 g). The proportions of the paths depend on the ratio v/V , while the size depends on A_{cent} and R_f .

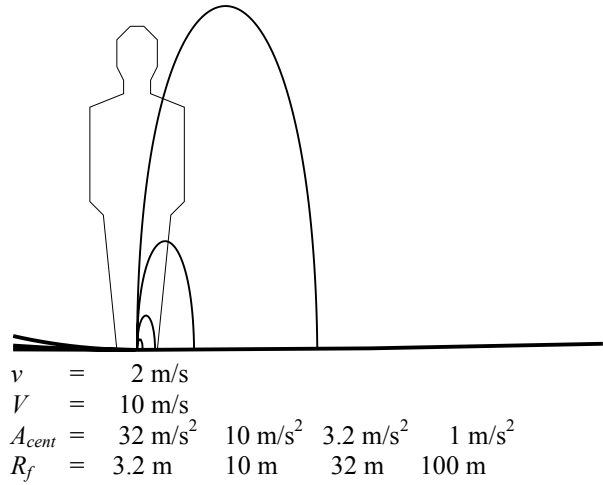


Figure 13. Hopping particles with an initial relative velocity v of 2 m/s and tangential velocity V of 10 m/s. The proportions of the paths depend on the ratio v/V , while the size depends on A_{cent} and R_f .

Figure 12 shows the relative paths of particles hopping with a certain initial relative velocity v , in artificial-gravity environments with a certain centripetal acceleration A_{cent} and a range of tangential velocities V . Holding A_{cent} constant while varying V requires varying R_f as well. The path heights are fairly consistent, as one might expect from the consistent A_{cent} value, but the proportions vary with the ratio v/V . The straighter, narrower proportions correspond to the smaller ratios.

Figure 13 is similar, but holds V constant while varying A_{cent} and R_f . The consistent ratio v/V results in consistent path proportions, but the size varies with A_{cent} and R_f .

The point of Figures 9 through 13 is to visualize the apparent artificial gravity field and its sensitivity to variations in the parameters A_{cent} , R_f , and V . As iron filings can delineate a magnetic field, so free-falling particles

can delineate a gravitational field. Contrary to the comfort charts, these figures reveal that there are no hard-edged boundary values where artificial gravity suddenly becomes Earth-like. Rather, the deviations from Earth-normalcy decrease as the radius and tangential velocity of the habitat increase, relative to the size and speed of the inhabitants.

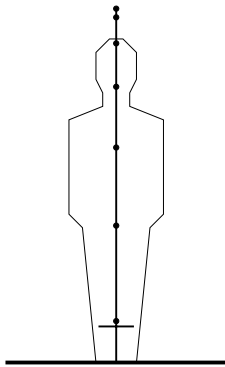


Figure 14. Earth gravity.

Figures such as these can help to visualize the significance of the comfort chart boundaries. But first, it's necessary to have a picture of normalcy as a basis for comparison. Figure 14 represents Earth-normal gravity. The dots represent particles dropping from an initial height of 2 m, spaced at time intervals of 0.1 s. The short horizontal line about 0.2 m above the floor marks the maximum height attained by a particle hopping from the floor with an initial velocity of 2 m/s. These values of $h = 2$ m and $v = 2$ m/s are within the envelope of common human activity and may serve as a standard for visualizing different gravity environments. Other values might serve as well, but these are convenient for now.

There is nothing remarkable about Figure 14, and there should not be, since it represents perhaps the most common of all human experiences: Earth gravity. It is the “gold standard” for gravity against which the next figure is to be evaluated.

Figure 15 is a reconstruction of Hill's and Schnitzer's comfort chart (chosen not because it's necessarily the best, but merely because it seems to be the most famous). The five boundary points of the proposed comfort zone are labeled as “a”, “b”, “c”, “d”, and “e”. For each of those points, Figure 15 includes a “hop and drop” diagram of artificial gravity under those conditions. The diagrams represent the same two particle tests: dropping from an initial height of 2 m, and hopping up from the floor with an initial velocity of 2 m/s. The deviations of these diagrams from the normalcy depicted in Figure 14 shows clearly that conformance to the comfort zone does not guarantee an Earth-like gravitational environment.

Point “a” in Figure 15 is the most like Earth. Besides a full “g” of acceleration, it provides a large radius and fast tangential velocity, yielding small ratios of h/R_f and v/V . This comes at a price: this is the point that demands the greatest investment in mass and kinetic energy for any particular material and structural configuration. (Mass is proportional to volume; kinetic energy is proportional to mass and tangential velocity squared.)

Point “b” also offers a full “g” of acceleration, so both the hop and the drop are comparable to their counterparts at point “a” with regard to speed and height. (The dots represent time intervals of 0.1 s.) However, this point pushes angular velocity to the maximum acceptable value in order to reduce the radius and tangential velocity, yielding larger ratios of h/R_f and v/V . Consequently, both the hop and the drop are more deviant.

Point “c” further reduces radius and tangential velocity to their minimum acceptable values, yielding still larger ratios of h/R_f and v/V and more deviant paths for both the hop and the drop. Because angular velocity is already at its maximum allowed value, reducing the radius also reduces the centripetal acceleration. Consequently, the hop is higher and the drop is slower. In contrast to point “a”, point “c” represents the minimum investment in mass and kinetic energy. The economic incentive to minimize these costs might contribute to the disparity of opinion, revealed back in Figure 6, regarding the location of this point. There is pressure to push the envelope here, but disagreement in how far it can be pushed while still maintaining some semblance of “comfort”.

Point “d” maintains the same minimum tangential velocity while also reducing acceleration to its minimum comfortable (or useful) value. This reduces angular velocity and the dizziness it induces, and increases radius. Due to the lower acceleration but equal ratio of v/V , the hop at “d” is higher but has the same proportions as at “c”. Due to the lower acceleration but also smaller ratio of h/R_f , the drop at “d” is slower but straighter than at “c”.

Point “e” maintains the same minimum acceleration while increasing radius to a large value. This further reduces the angular velocity while it increases the tangential velocity. The hops at “d” and “e” are comparable in height, due to the equal acceleration. The proportions at “e” are narrower than “d”, but wider than “a”, due to the intermediate tangential velocity and v/V ratio. The drop at “e” is as slow as “d” due to the equal acceleration, but as straight as “a” due to the equal radius and h/R_f ratio.

Of these five boundary points, “c” demands the closest scrutiny because it seeks to minimize obvious costs in radius, tangential velocity, mass, and kinetic energy, but incurs less-obvious costs in design, crew selection, training, and acclimatization to accommodate the peculiar gravitational environment. Moreover, as illustrated in Figure 6, there is considerable disagreement regarding the coordinates of this point.

Figure 16 explores the significance of this disagreement. For each of the five comfort charts cited back in Section II, Figure 16 overlays a hop-and-drop diagram for the boundary point at the proposed minimum radius and tangential velocity. Comparisons such as this help to reveal the extent to which the various authors push the bounds of the comfort zone. Ultimately, designers need to decide who to believe and which set of criteria to follow. Even the most conservative criteria allow for considerable deviation from Earth-like gravity.

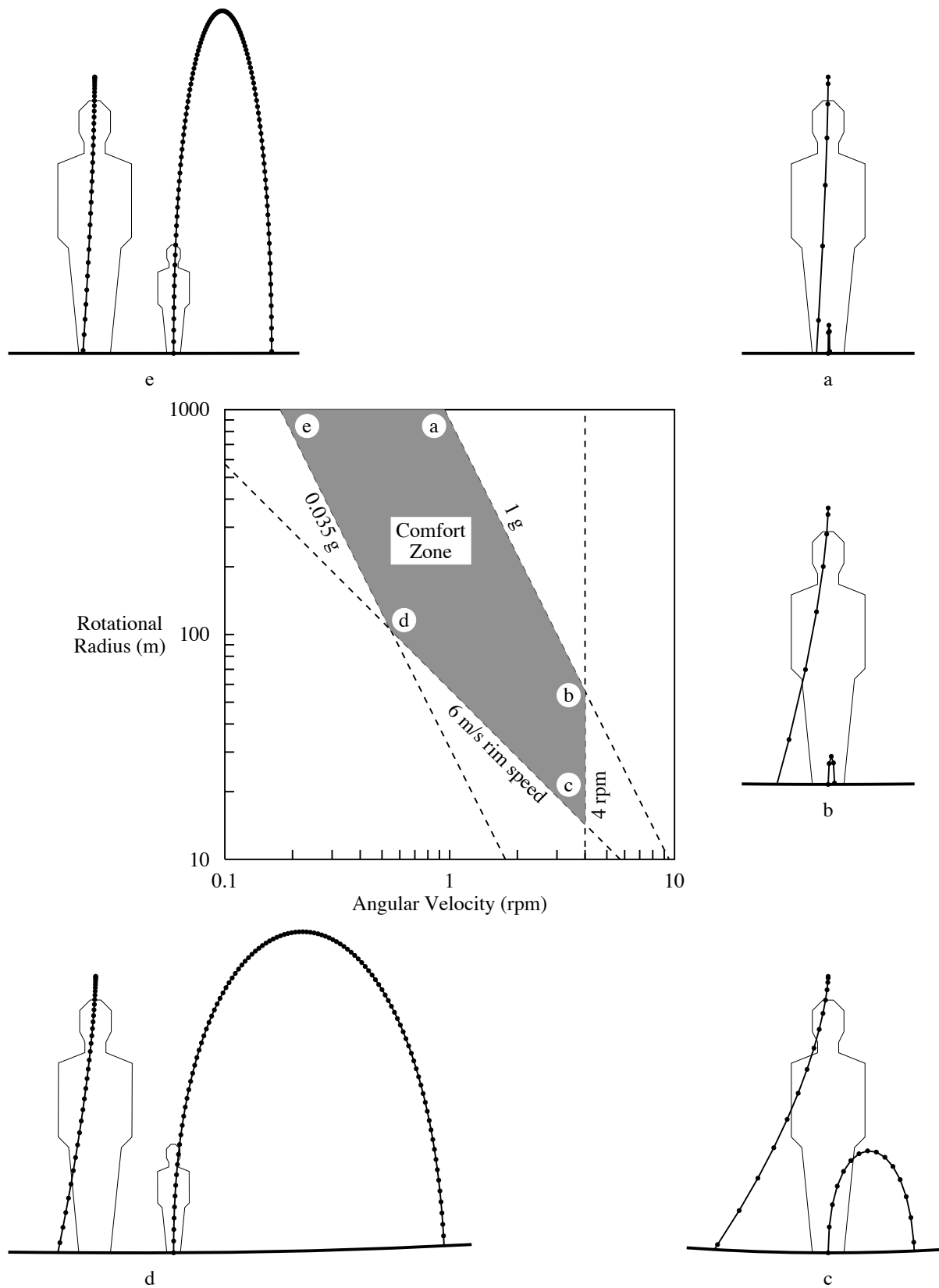


Figure 15. Artificial gravity at the boundary points of the comfort zone.

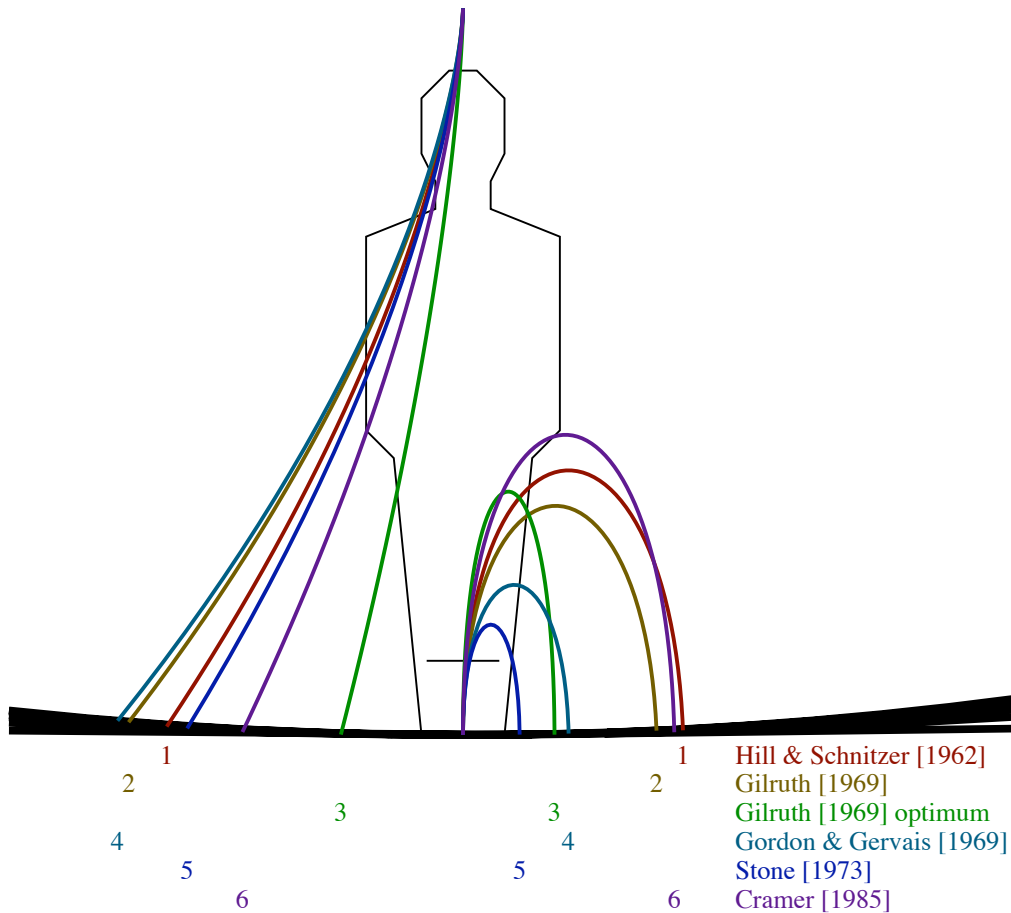
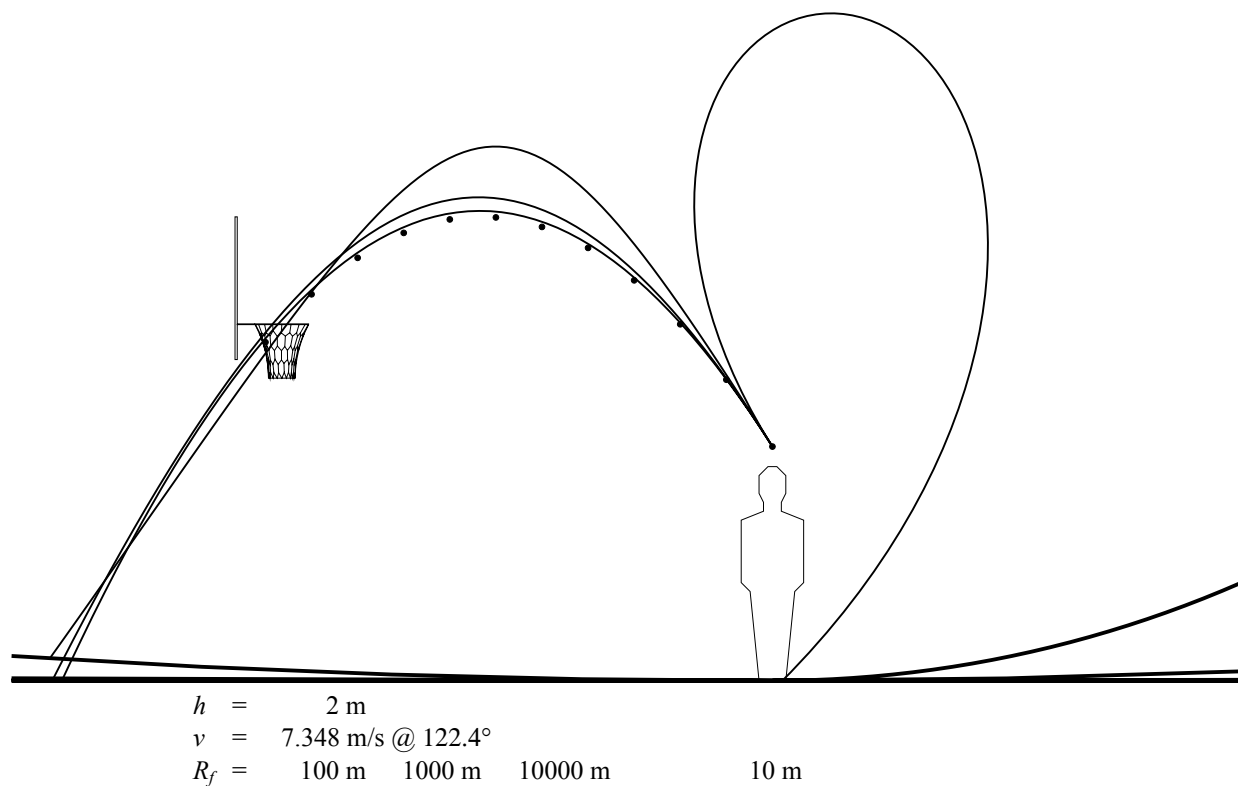


Figure 16. Artificial gravity at the minimum “comfortable” radius and tangential velocity proposed by various authors.

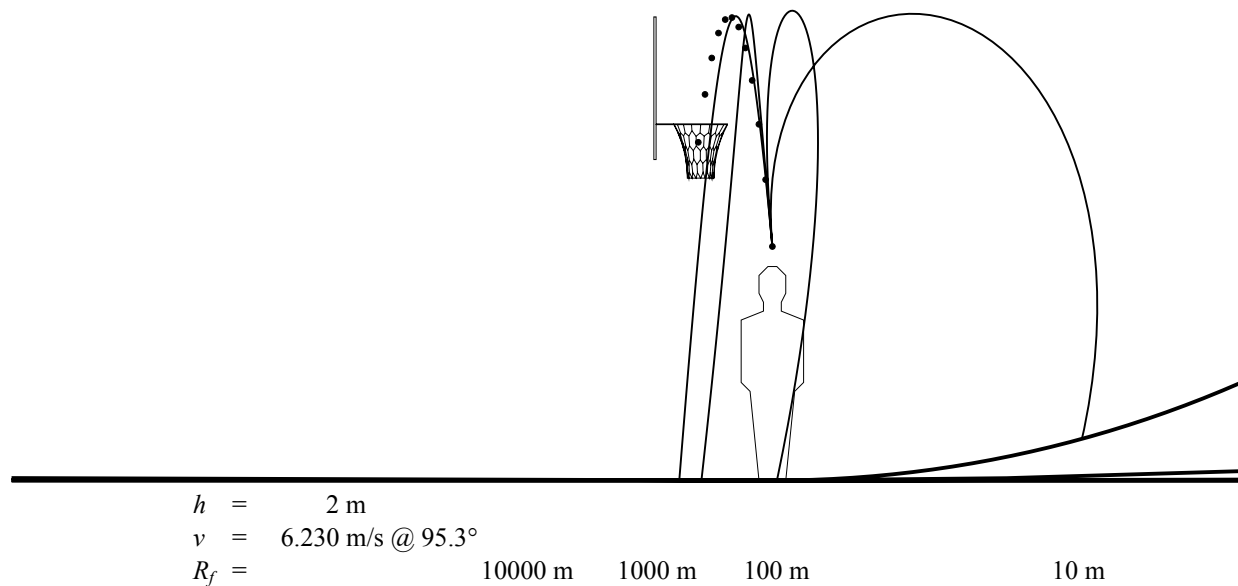
The use of standard tests such as a 2-meter drop and a 2-meter-per-second hop are useful for comparing gravitational environments in a generic way. Any criteria that represent the envelope of common human activities could serve as well. Nevertheless, such tests might not be sufficient. It's necessary also to visualize specific activities that are important to a particular situation.

To illustrate this point, Figure 17 uses basketball as an example. This simple simulation abstracts the ball to a particle at the ball's center (ignoring any effects of its spin, drag, elasticity, and so on). Similarly, it abstracts the player to a mannequin, included only to indicate scale (ignoring all of the complexities of human kinematics). The dots represent a successful shot in Earth gravity. The curves represent the paths of particles thrown in precisely the same manner in 1 g rotating environments with radii of 10 m, 100 m, 1000 m, and 10000 m. The artificial gravity in the 10 m environment is so distorted that the particle turns backward and falls behind the shooter. None of the cited authors regard this environment as comfortable. From the free-throw line, the shots in the 100 m, 1000 m, and 10000 m environments appear to hit. (The goal would need to be rotated up slightly to account for the floor curvature.) But closer to the net, the shot in the 100 m environment also turns backward, and even in the 1000 m environment the particle misses the goal. This implies that terrestrial players may need to make subtle adjustments in their technique when visiting space colonies as large as the Stanford Torus or the Bernal Sphere [Johnson, Holbrow, 1977]. In smaller space hotels, the rules of the game itself might need substantial revision.

Figure 17 shows only the “west” goal, with the player shooting up and *against* the environment's tangential velocity. The effects would be different at the “east” goal, shooting *with* the tangential velocity. Switching goals at the start of each period might cancel any advantage of one goal over the other. Turning the court's orientation from east-west to north-south – parallel to the axis of rotation – might also eliminate any such advantage. However, this would not eliminate the gravitational deviations, but would merely orient them in the plane of the backboard instead of perpendicular to it. One goal would be biased toward the left, the other toward the right.



a. Shooting from the free-throw line.



b. Shooting from close under the net.

Figure 17. Basketball in artificial gravity. The dots represent a successful shot in Earth gravity. The curves represent identical shots in 1-g rotating environments with radii of 10 m, 100 m, 1000 m, and 10000 m.

IV. Apparent Slopes and Catenary Curves

As Figures 9 through 13 illustrate, a particle moving at constant velocity in an inertial frame of reference appears to change velocity in a rotating frame of reference. Conversely, a particle that appears to move at constant velocity in the rotating frame must undergo a change of velocity in the inertial frame. Any change in either its speed or direction constitutes acceleration. This is the afore-mentioned Coriolis acceleration. Its magnitude and direction are determined by the vector cross product of the environment's angular velocity Ω (radians per time) and the particle's relative linear velocity \mathbf{v} (distance per time) in the rotating frame:

$$\mathbf{A}_{Cor} = 2 \cdot \Omega \times \mathbf{v}$$

As a cross product, the Coriolis acceleration is perpendicular to both the axis of rotation and the relative velocity, with a magnitude proportional to the sine of the angle between them. For velocity parallel to the axis, the Coriolis acceleration is zero. For velocity perpendicular to the axis (in the plane of rotation), its magnitude is simply:

$$A_{Cor} = 2 \cdot \Omega \cdot v$$

Constant relative velocity in the rotating frame requires Coriolis acceleration in the inertial frame, and this contributes, along with the centripetal acceleration, to the total apparent gravity. This is especially important to walking on flat floors and climbing straight ladders.

Figure 18 shows the situation for an observer walking east (prograde) on a flat floor in rotating environment. The floor is a chord of a circle, with its midpoint at radius R_c from the center of rotation. The observer's centripetal acceleration is always toward the center; its magnitude and direction depend only on his position, independent of his relative speed. On the other hand, his Coriolis acceleration depends only on his relative speed, independent of his position. The total acceleration, $\mathbf{A} = \mathbf{A}_{cent} + \mathbf{A}_{Cor}$, determines his net apparent gravity and sense of "up". At the center of the chord, its magnitude is:

$$\begin{aligned} A &= A_{cent} + A_{Cor} \\ &= \Omega^2 \cdot R_c + 2 \cdot \Omega \cdot v \\ &= \Omega^2 \cdot (R_c + 2 \cdot v / \Omega) \end{aligned}$$

So, the Coriolis component effectively raises the convergence point for the net acceleration by $2 \cdot v / \Omega$ from the center of rotation.

Figure 19 shows what happens when the observer reverses direction and walks back west (antigrade). The Coriolis acceleration also reverses direction, thereby lowering the convergence point.

In Figures 18 through 21, the x,y coordinate axes are tied to the rotating environment. The observer carries his own coordinate axes with him, tied to his sense of horizontal and vertical, determined by his net acceleration. These axes are labeled ξ, η . The apparent slope of the floor changes with respect to these axes as the observer walks across it.

Figures 20 and 21 show the situation from the observer's point of view. Though the floor looks straight, it seems to teeter-totter across a hill. Both the shape of the apparent hill and the magnitude of the apparent gravity follow catenary curves [Hall, 1999]:

$$\begin{aligned} \eta/q &= -\cosh(\xi/q) \\ A/q &= \Omega^2 \cdot \cosh(\xi/q) \\ q &= R_c + 2 \cdot v / \Omega \end{aligned}$$

The dotted lines in Figures 19 through 21 represent the magnitude and direction of the apparent gravity. Compared to eastward motion, in westward motion the hill is steeper but the gravity is weaker.

Figures 22 and 23 illustrate ascending a "vertical" ladder that passes through the center of rotation. In this case, R_c is zero. Although the centripetal acceleration is zero at the center point, the Coriolis acceleration remains constant and non-zero as long as the observer continues to ascend at constant velocity.

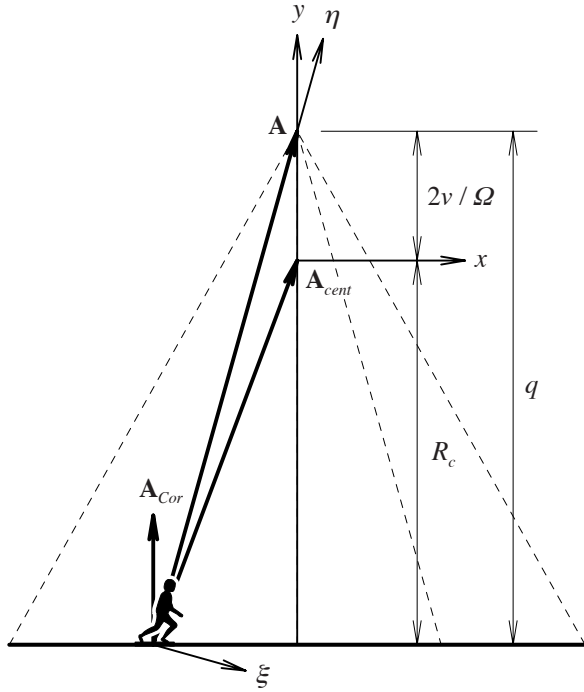


Figure 18. Walking east on a flat floor.

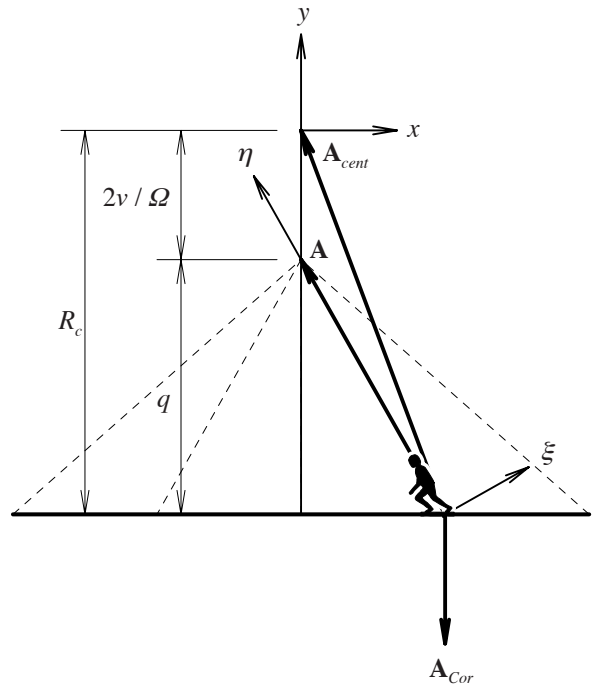


Figure 19. Walking west on a flat floor.

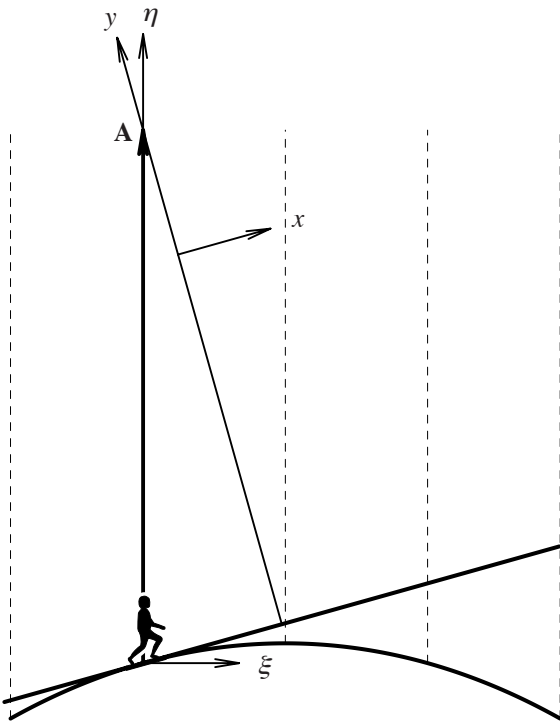


Figure 20. Apparent slope while walking east.

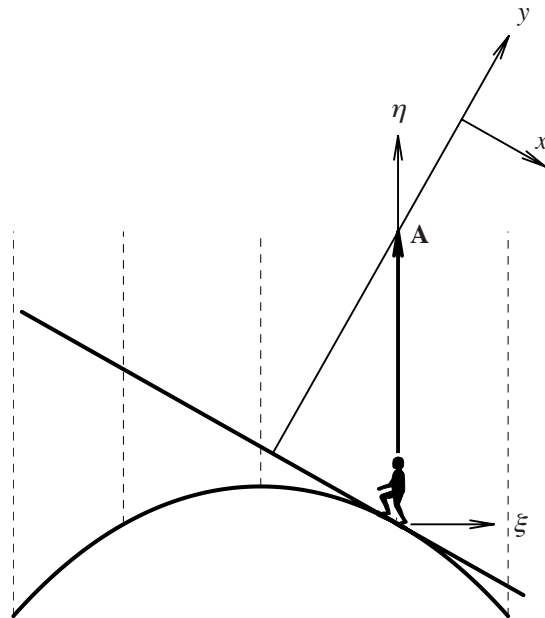


Figure 21. Apparent slope while walking west.

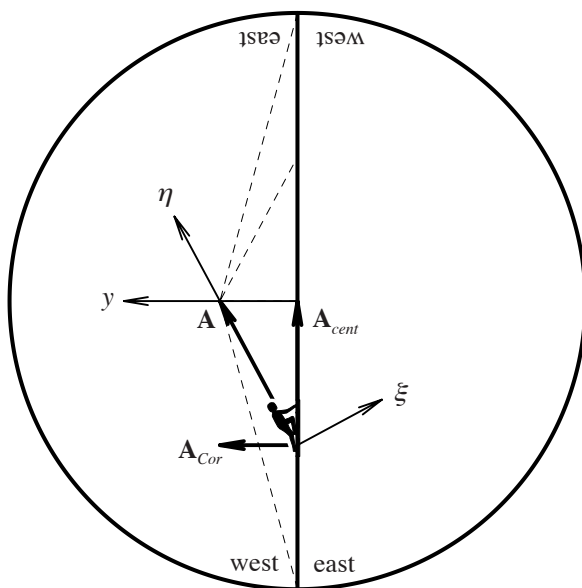


Figure 22. Ascending a ladder.

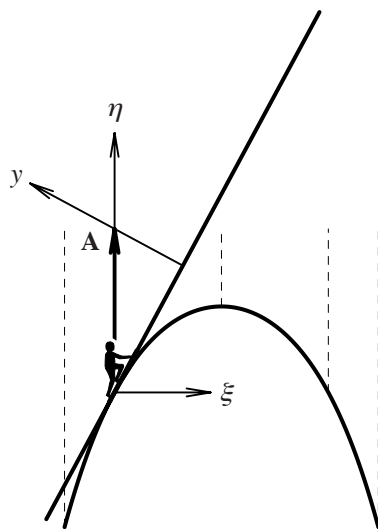


Figure 23. Apparent slope while ascending.

It's the stiffness of the ladder that provides the observer's Coriolis acceleration by constraining him to straight-line motion in the rotating frame. As he ascends toward the center, the ladder decreases his tangential velocity; as he descends toward the perimeter, the ladder increases his tangential velocity. To stay above the curve, it's essential that he ascend on the west side, as shown, and descend on the east side, so that the ladder presses toward him. If he attempts to climb on the wrong side, the ladder will pull away from him, as if he were climbing on the underside of the curve. It's difficult enough to climb a truly vertical ladder. A ladder that leans backward is not only uncomfortable, but unsafe. For the designer, this raises several key points:

- The plane of the ladder should be parallel to the axis of rotation, perpendicular to the plane of rotation and to the Coriolis acceleration.
- Either the ladder should be accessible from both sides, or separate ladders (accessible from opposite sides) should be provided for ascending and descending. Figure 24 illustrates three possibilities.
- It would be even better to avoid ladders entirely, by leaning the line of motion far enough away from the center of rotation so that it functions as a stair.

Will these floor and ladder slopes be “apparent” in any real implementation, or are they only theoretical? Figures 25 and 26 address this question by considering a multi-storey module similar to TransHab [Kennedy, 1999] in an artificial-gravity application. Its top floor is at the minimum radius and tangential velocity that satisfies all of the comfort criteria cited in Section II – about 67.1 m and 14.0 m/s, respectively. Figure 25 shows an observer walking west on the top level at a modest speed of about 1 m/s, while Figure 26 shows him descending from that level at 0.5 m/s. Once again, these figures show that even the most conservative criteria allow for considerable deviation from Earth-like gravity. The floor's maximum apparent slope is nearly 4° (about a 7% grade, or 1:15). The ladder's apparent lean from vertical is also about 4°. These deviations would be even greater with faster walking and climbing speeds, a wider floor, a shorter radius, or a slower tangential velocity – which most renditions of the comfort zone allow.

Published illustrations of artificial-gravity habitats often fail to account for these effects. For example, Figure 27 shows two scenes from a computer animation of a TransHab module in an artificial-gravity crew transfer vehicle [Borowski, Dudzinski, Sauls, Minsaas, 2006]. To provide 0.38 g at 4 rpm, the top level would have a rotational radius of only about 21.2 m and a tangential velocity of 8.9 m/s. Although these values are within most renditions of the comfort zone, they are much less than the values assumed in Figures 25 and 26. Consequently, the floor would seem considerably more sloped – as much as 13° (23% grade, 1:4.33) for westward motion at 1 m/s and 3.8 m from the centerline. The ladder at this level would seem to lean more than 6° from vertical for descent at 0.5 m/s. It's not clear how the ladder in this movie is oriented with respect to the rotation, but it is clear that there is only one ladder and it cannot function well for both ascending and descending.

Figure 28 is a scene from the movie *2001: A Space Odyssey* [Kubrick, Clarke, 1968], showing a crewman descending a ladder in the side wall of the rotating section of a spacecraft. The floor radius is about 5.33 m and it rotates at about 5.3 rpm to simulate Lunar gravity. Under these conditions, if he descends at 0.5 m/s, the apparent

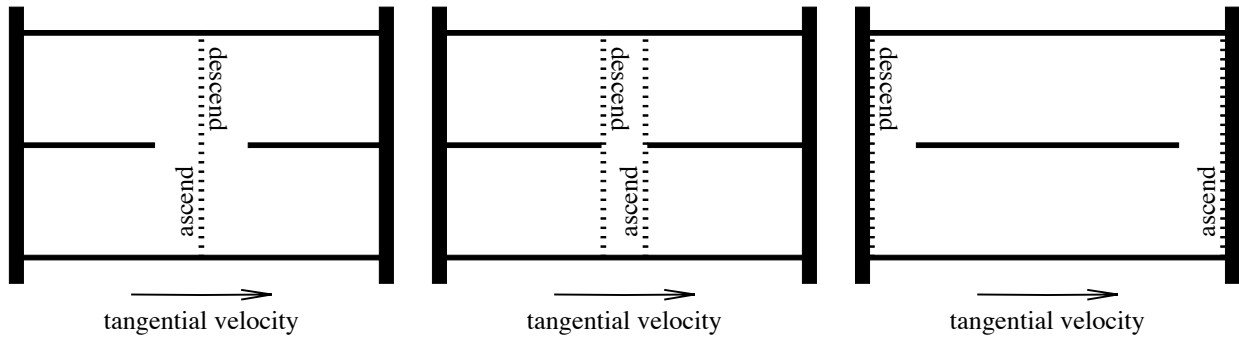


Figure 24. Three recommended options for orienting ladders in artificial gravity.

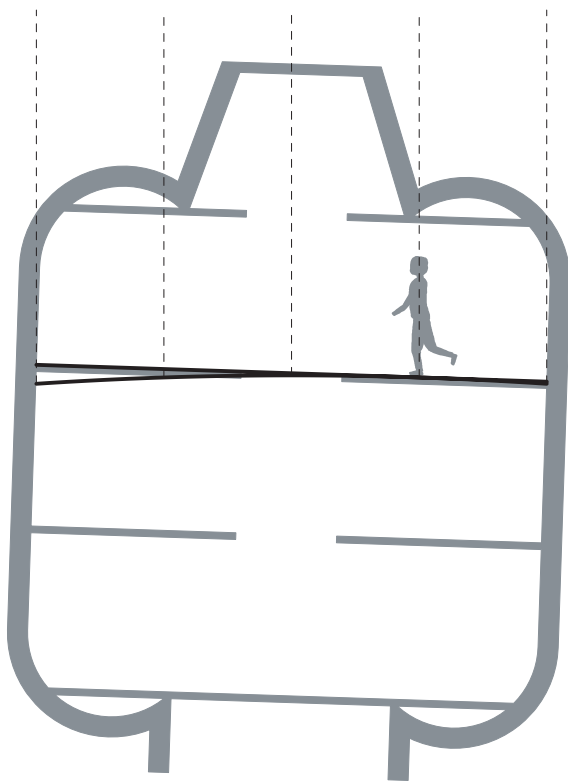


Figure 25. Walking west at 1 m/s on a flat floor rotating at radius 67.1 m and tangential velocity 14.0 m/s. This is the minimum radius and tangential velocity that satisfies all of the cited comfort criteria. The apparent floor slope at the wall is nearly 4° (about a 7% grade, or 1:15).

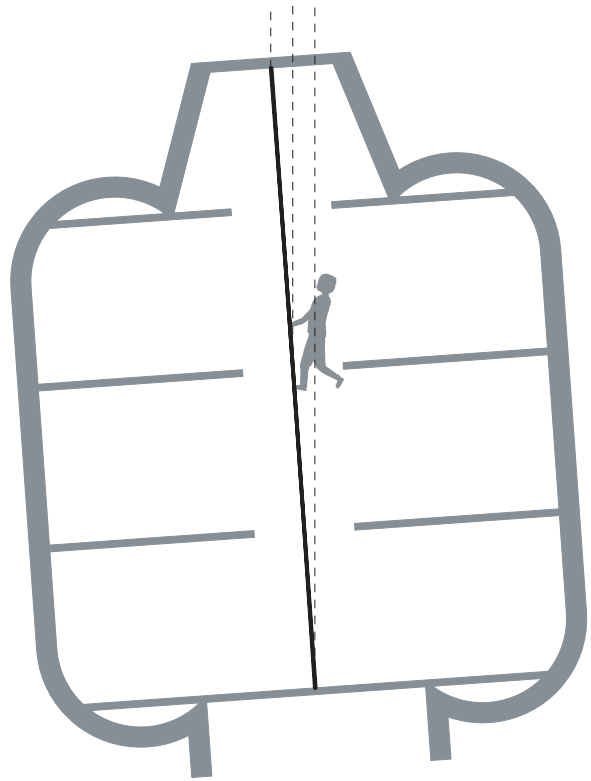


Figure 26. Descending a ladder at 0.5 m/s on a “vertical” ladder rotating at radius 67.1 m and tangential velocity 14.0 m/s. This is the minimum radius and tangential velocity that satisfies all of the cited comfort criteria. The apparent lean of the ladder is 4° from vertical.



Figure 27. Scenes from a computer animation of a TransHab module in an artificial-gravity crew transfer vehicle. From the “Bimodal NTR Artificial Gravity Mars Mission” produced by NASA Glenn Research Center and John Frassanito & Associates [Borowski, Dudzinski, Sauls, Minsaas, 2006]. With 0.38 g at 4 rpm, the top floor radius would be 21.2 m with a tangential velocity of 8.9 m/s. Under these conditions, the apparent floor slope when walking west at 1 m/s would be as much as 13° (23% grade, 1:4.33). The apparent lean of the ladder when descending at 0.5 m/s would be more than 6° from vertical. Due to the reversal of Coriolis acceleration in ascending versus descending, one ladder cannot provide safe transit in both directions.



Figure 28. Descending a ladder in the side wall of a rotating spacecraft section. From the movie *2001: A Space Odyssey* [Kubrick, Clarke, 1968].

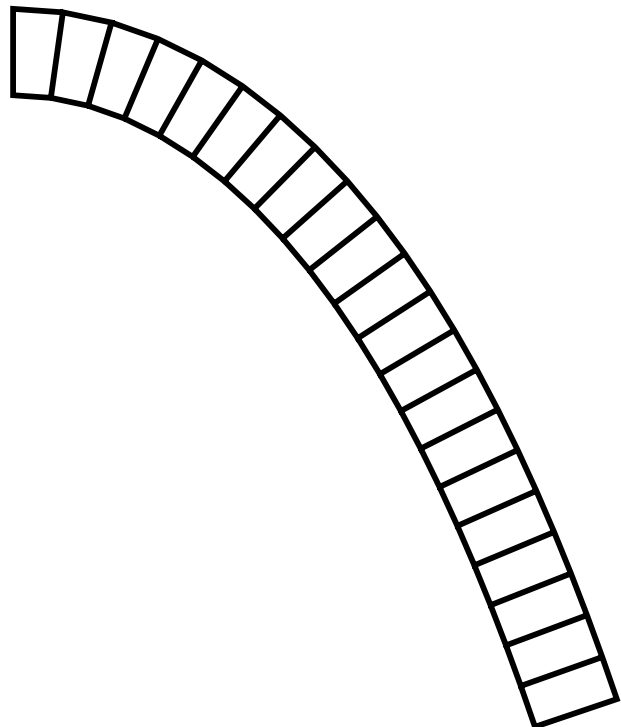


Figure 29. The apparent lean of the ladder in Figure 28, due to the lateral Coriolis acceleration.

lean of the ladder will be as depicted in Figure 29. The Coriolis acceleration acts in the plane of the ladder, instead of perpendicular to it, and near the center it's proportionally much greater than the centripetal acceleration. The effect is as if the ladder was bent over on its side. The ladder should be turned perpendicular to the side wall so that it acts more like a ramp.

Figure 30 is a detail from an illustration of a "variable gravity research station" published in the proceedings of the 3rd "Case For Mars" conference [Staehle, 1989]. It shows a ladder oriented coplanar with large external dishes that seem to be aimed at a fixed target. If the dishes maintain a fixed orientation, then they and the ladder must be coplanar with the rotation. This ladder, similar to the one in Figures 28 and 29, will seem to lean sideways in relation to the Coriolis acceleration. The danger may be exacerbated by the flow of blood away from the brain as a person descends into stronger centripetal acceleration. If there must be a ladder, then it should at least be turned 90° in the plan, to place it perpendicular to the Coriolis acceleration. A series of stairs would be considerably safer.

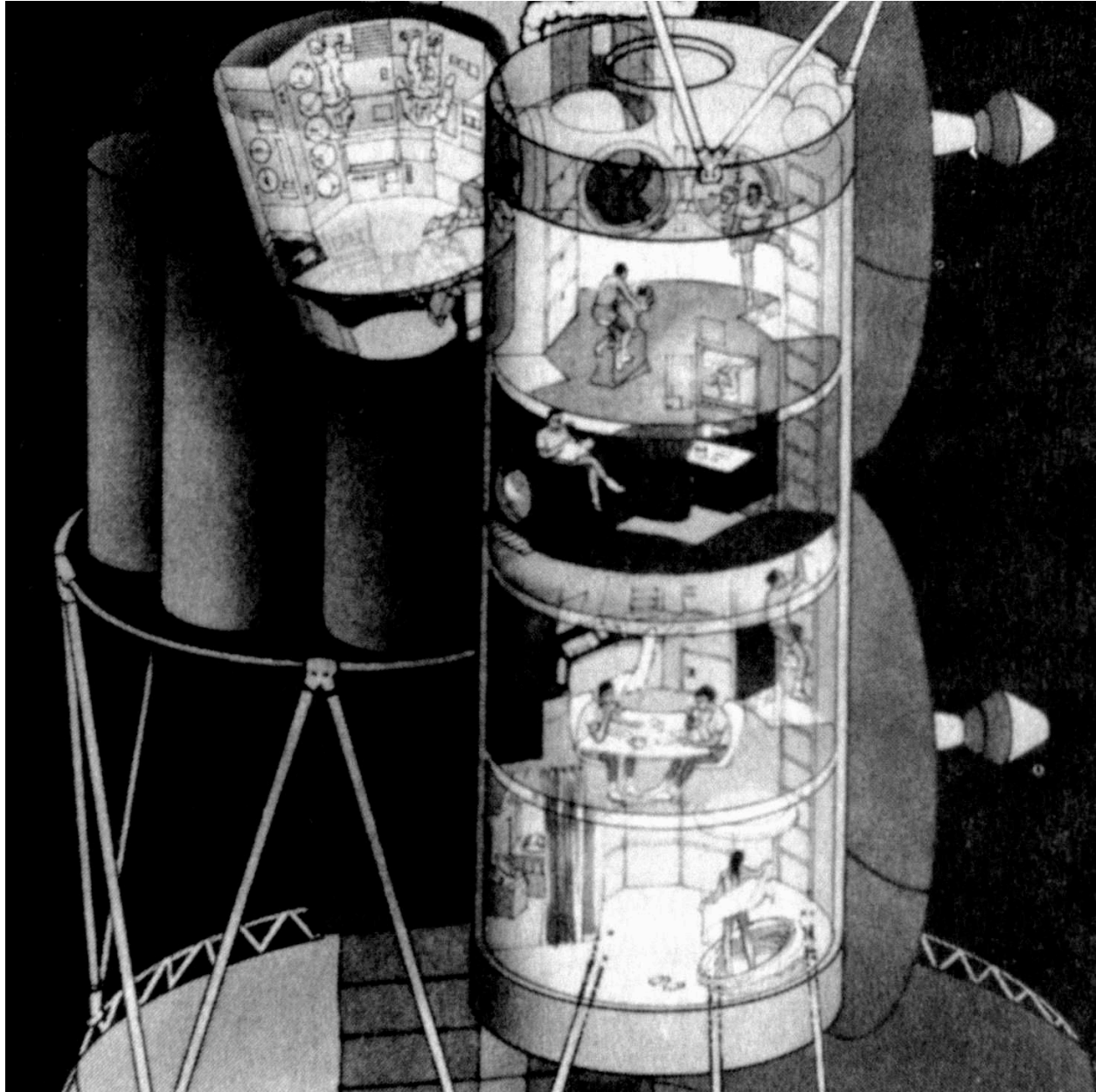


Figure 30. Climbing a ladder in the side wall of a variable gravity research station. Detail from an illustration by Carter Emmart for the 3rd "Case for Mars" conference [Staehle, 1989]. Similar to Figures 28 and 29, this ladder will seem to lean sideways unless it's turned 90° in the plan.

V. Computer Aided Design and Virtual Reality for Artificial-Gravity Visualization

Computer aided design (CAD) can be a powerful tool for simulating and testing environments before they're built. However, as with all tools, it's the responsibility of the craftsman to use them skillfully: the best hammers and saws in the world won't compensate for an unskilled or careless carpenter. Several common CAD systems provide the means for computing walk-throughs and other kinds of animations. Some of these systems are capable of rendering particle physics, with realistic rules for force, mass, acceleration, velocity, and momentum. The onus is on the designer and renderer to use these tools with understanding and skill.

Simple key-frame animations, with built-in erroneous assumptions about the gravitational environment, cannot be used to visualize or validate a design for artificial gravity. An animation with realistic rendering of light and material and articulated human figures, but without regard to the actual physics of rotating systems, is actually detrimental. To the extent that such an animation lulls viewers into unrealistic expectations of mobility in artificial gravity, it's worse than no visualization at all.

A human body is a complicated mechanism, and realistic simulation of its articulations is difficult to achieve. A common approach to life-like animation is to record body segment positions and rotations from an actor performing various tasks in a studio, then apply these data to a geometric model of a human or some other creature. Because the effects of Earth gravity are implicit in the recorded data, the data are not valid for predicting mobility in any other gravitational environment.

Human mobility is a complex interaction of muscular force, body segment mass and distribution, inertia, gravitation, and the acceleration of the frame of reference. A robust, predictive simulation, adequate for validating a new gravitational environment, must account for all of these factors by applying the laws of physics to an accurate and detailed anthropometric model. This is the realm of "digital human modeling," and there is a considerable body of research, data, and software to support it. Anyone aiming to validate an artificial-gravity environment through computed human animation must enter this realm. If a lack of resources precludes this, then design integrity is better served by simple yet physically accurate particle simulations rather than visually stunning but physically flawed cartoons.

Immersive, high-fidelity, virtual-reality simulations could be very powerful for exploring certain aspects of artificial-gravity design. Unfortunately, the accessibility of such simulations tends to be inversely proportional to their sophistication. The most sophisticated simulation in the world is no help to those who have no access to it. The visualizations presented in this paper are intended for easy accessibility here and now. They do not preclude development of other more sophisticated visualizations. In fact, they aim to encourage it. Again, it must be stressed that high-tech virtual reality systems are superb at visualizing imaginary environments that defy the laws of physics. It is the designer's responsibility to use these tools with knowledge and integrity.

VI. Conclusion

In planning artificial gravity environments, reducing radius and tangential velocity reduces obvious costs in mass and kinetic energy. Less obvious are the potential cost increases to accommodate a distorted gravitational environment. At the outset, these ought to include a greater investment in design – including research, testing, and scrupulous review of assumptions carried over from terrestrial experience. Other cost increases might include more stringent crew selection, longer periods of training and acclimatization, and reduced crew productivity. Highly-skilled candidates for an interplanetary expedition might be disqualified by physiological intolerance and inability to adapt to conditions at the edge of the comfort zone for rotation.

The habitat pressure shell does not shield the interior from physics and mechanical dynamics. The same concerns that govern the overall configuration of a rotating spacecraft must be brought to bear on the interior architecture. In an artificial-gravity environment, the direction of rotation should be visually obvious in the design: to orient movements advantageously with regard to Coriolis accelerations; and to establish a connection between visual and vestibular cues to rotation. If the rotation isn't apparent in the design, that's an indication that it wasn't important to the designer.

Floors that are wide with respect to the rotational radius should not be flat. They should be cylindrical arcs so that the centripetal acceleration is always perpendicular to the surface, thus avoiding unwanted apparent slopes.

Circular plans with no obvious orientation to the habitat's rotation should be discarded. If other design considerations mandate a vertical cylindrical habitat, the interior should nevertheless be laid out on a grid aligned with the axis of rotation (north-south) and tangential velocity (east-west). Much as the cylindrical modules of the International Space Station are inscribed with a square living space with distinct identifiable wall, floor, and ceiling surfaces, so a module in artificial gravity should be inscribed with axis-aligned partitions, with distinct east, west,

north, and south walls, regardless of the module's exterior shape. Bending the floor into an arc, as suggested in the previous paragraph, will already begin to establish this orientation.

Color and pattern can be applied to further distinguish the east (fore, prograde) and west (aft, antigrade) directions. These can help to keep the inhabitants visually oriented with respect to the rotation, so that they can anticipate the direction of Coriolis acceleration that will accompany various actions such as standing up and sitting down.

Multistory designs should be avoided. If they're unavoidable, then vertical circulation must be planned with Coriolis acceleration as a principal consideration. The plane of a ladder should be parallel to the axis of rotation, so that the Coriolis acceleration is perpendicular to that plane. Moreover, upward and downward motion should be accommodated on opposite faces of the same ladder, or on opposite ladders, so that the acceleration always presses the ladder against the climber and never pulls it away.

In designing for artificial gravity, question all assumptions about gravity. This practically means, question everything.

References

- Borowski, Stan; Dudzinski, Len; Sauls, Bob, Minsaas, Lars (2006). "Bimodal NTR Artificial Gravity Mars Mission." NASA Glenn Research Center and John Frassanito & Associates.
<http://www.lunar-rocket.com/flash.html>
- Clark, Carl C.; Hardy, James D. (1960). "Gravity Problems in Manned Space Stations." In, *Proceedings of the Manned Space Stations Symposium* (p. 104-113). Los Angeles, California, USA, 20-22 April 1960. New York, New York, USA: Institute of the Aeronautical Sciences.
- Cramer, D. Bryant (1985). "Physiological Considerations of Artificial Gravity." In A. C. Cron (Ed.), *Applications of Tethers in Space* (NASA CP-2364, vol. 1, p. 3-95-3-107). Workshop held in Williamsburg, Virginia, USA, 15-17 June 1983. Washington, DC, USA: National Aeronautics and Space Administration.
- Gilruth, Robert R. (1969). "Manned Space Stations – Gateway to Our Future in Space." In S. F. Singer (Ed.), *Manned Laboratories in Space* (p. 1-10). New York, New York, USA: Springer-Verlag.
- Gordon, Theodore J.; Gervais, Robert L. (1969). "Critical Engineering Problems of Space Stations." In S. F. Singer (Ed.), *Manned Laboratories in Space* (p. 11-32). New York, New York, USA: Springer-Verlag.
- Hall, Theodore W. (1999 September). *Inhabiting Artificial Gravity* (AIAA 99-4524). AIAA Space Technology Conference and Exposition, Albuquerque, New Mexico, USA, 28-30 September 1999. Reston, Virginia, USA: American Institute of Aeronautics and Astronautics.
- Hill, Paul R.; Schnitzer, Emanuel (1962 September). "Rotating Manned Space Stations." *Astronautics*, vol. 7, no. 9, p. 14-18. New York, New York, USA: American Rocket Society.
- Johnson, Richard D.; Holbrow, Charles (Eds.) (1977). *Space Settlements: A Design Study* (NASA SP-413). Washington, DC, USA: National Aeronautics and Space Administration.
<http://www.nas.nasa.gov/About/Education/SpaceSettlement/75SummerStudy/Design.html>
- Kennedy, Kriss J. (1999 July). *ISS TransHab: Architecture Description* (SAE 1999-01-2143). 29th International Conference on Environmental Systems (ICES), Denver, Colorado, USA, 12-15 July 1999. Warrendale, Pennsylvania, USA: Society of Automotive Engineers.
- Kubrick, Stanley; Clarke, Arthur C. (1968). *2001: A Space Odyssey*. Hollywood, California, USA: Metro-Goldwyn-Mayer.
- NASA (1995 July). *Man-Systems Integration Standards, Revision B* (NASA STD-3000), vol. 1, sec. 5.3.2.3. Washington, DC, USA: National Aeronautics and Space Administration.
http://msis.jsc.nasa.gov/sections/section05.htm#_5.3_ACCELERATION
- Schultz, David N.; Rupp, Charles C.; Hajos, Gregory A.; Butler, John M. (1989). *A Manned Mars Artificial Gravity Vehicle* (AAS 87-203). In C. Stoker (Ed.), *The Case for Mars III: Strategies for Exploration – General Interest and Overview* (American Astronautical Society, Science and Technology Series, Vol. 74, p. 325-352). Boulder, Colorado, USA, 18-22 July 1987. San Diego, California, USA: Univelt, Inc.
- Staehle, Robert L. (1989). *Earth Orbital Preparations for Mars Expeditions* (AAS 87-205). In C. Stoker (Ed.), *The Case for Mars III: Strategies for Exploration – General Interest and Overview* (American Astronautical Society, Science and Technology Series, Vol. 74, p. 373-396). Boulder, Colorado, USA, 18-22 July 1987. San Diego, California, USA: Univelt, Inc.
- Stone, Ralph W. (1973). "An Overview of Artificial Gravity." In, *Fifth Symposium on the Role of the Vestibular Organs in Space Exploration* (NASA SP-115, p. 23-33). Pensacola, Florida, USA, 19-21 August 1970. Washington, DC, USA: National Aeronautics and Space Administration.
- Tillman, Barry (1987). "Human Factors in the Design of an Artificial Gravity Research Facility." Unpublished report prepared under contract for Lockheed Missile and Space Company, Sunnyvale, California, USA.